The Journal of Immunology

Myeloid PTEN Deficiency Protects Livers from Ischemia Reperfusion Injury by Facilitating M2 Macrophage Differentiation

Shi Yue, Jianhua Rao, Jianjun Zhu, Ronald W. Busuttil, Jerzy W. Kupiec-Weglinski, Ling Lu, Xuehao Wang and Yuan Zhai

References	This article **cites 45 articles**, 14 of which you can access for free at: http://www.jimmunol.org/content/192/11/5343.full#ref-list-1

Why *The JI*? Submit online.

- **Rapid Reviews! 30 days*** from submission to initial decision

- **No Triage!** Every submission reviewed by practicing scientists

- **Fast Publication!** 4 weeks from acceptance to publication

*average

Subscription	Information about subscribing to *The Journal of Immunology* is online at: http://jimmunol.org/subscription
Permissions	Submit copyright permission requests at: http://www.aai.org/About/Publications/JI/copyright.html
Email Alerts	Receive free email-alerts when new articles cite this article. Sign up at: http://jimmunol.org/alerts

Myeloid PTEN Deficiency Protects Livers from Ischemia Reperfusion Injury by Facilitating M2 Macrophage Differentiation

Shi Yue,*[,1] Jianhua Rao,*[,†,1] Jianjun Zhu,*[,‡] Ronald W. Busuttil,*
Jerzy W. Kupiec-Weglinski,* Ling Lu,[†] Xuehao Wang,[†] and Yuan Zhai*

Although the role of phosphatase and tensin homolog deleted on chromosome 10 (PTEN) in regulating cell proliferation is well established, its function in immune responses remains to be fully appreciated. In the current study, we analyzed myeloid-specific PTEN function in regulating tissue inflammatory immune response in a murine liver partial warm ischemia model. Myeloid-specific PTEN knockout (KO) resulted in liver protection from ischemia reperfusion injury (IRI) by deviating the local innate immune response against ischemia reperfusion toward the regulatory type: expression of proinflammatory genes was selectively decreased and anti-inflammatory IL-10 was simultaneously increased in ischemia reperfusion livers of PTEN KO mice compared with those of wild-type (WT) mice. PI3K inhibitor and IL-10–neutralizing Abs, but not exogenous LPS, recreated liver IRI in these KO mice. At the cellular level, Kupffer cells and peritoneal macrophages isolated from KO mice expressed higher levels of M2 markers and produced lower TNF-α and higher IL-10 in response to TLR ligands than did their WT counterparts. They had enhanced Stat3- and Stat6-signaling pathway activation, but diminished Stat1-signaling pathway activation, in response to TLR4 stimulation. Inactivation of Kupffer cells by gadolinium chloride enhanced proinflammatory immune activation and increased IRI in livers of myeloid PTEN KO mice. Thus, myeloid PTEN deficiency protects livers from IRI by facilitating M2 macrophage differentiation.   *The Journal of Immunology*, 2014, 192: 5343–5353.

T oll-like receptor 4 activation has been identified in recent years as the key initiating step of the liver inflammatory immune response against ischemia reperfusion (IR) (1–3). Because both pro- and anti-inflammatory gene programs are triggered downstream of TLR4 engagement via multiple intracellular-signaling pathways (4, 5), the question of whether we can manipulate TLR-signaling pathways to curtail its tissue-damaging proinflammatory property is of high interest to identify potential therapeutic targets. The PI3K/Akt–signaling pathway was shown to be an endogenous gate-keeping system to prevent excessive innate immune responses (6). Mice deficient in the PI3K regulatory subunit

showed enhanced Th1 responses as the result of increased IL-12 production from dendritic cells (DCs) (7). More recent studies revealed that glycogen synthase kinase 3β (Gsk3β) represents a key target of this negative-regulatory pathway of TLR responses (8, 9). As a constitutively active kinase, Gsk3β is inactivated upon innate immune stimulation in macrophages by Akt, and Gsk3 inhibition results in diminished NF-κB–driven proinflammatory, but increased IL-10, gene expression (8, 10). We showed that active Gsk3β is critical for the liver proinflammatory immune response against IR, because its inhibitor SB216367 was able to shift the liver immune response toward an IL-10–dominated regulatory type and protected livers from IR injury (IRI) (11).

Because the PI3K/Akt/Gsk3β–signaling pathway is involved in multiple aspects of cellular functions in different cell types, including proliferation, differentiation, apoptosis, and chemotaxis (12, 13), the precise definition of its immune regulatory function in vivo in a complex organ, such as liver, requires cell type–specific analysis. In particular, the immune response against IR is triggered by tissue damage via damage-associated molecular patterns, and any regulatory mechanisms of parenchymal cell death will have indirect impacts on immune activation. Thus, non–cell-selective targeting approaches of this signaling pathway, such as chemical inhibitors of PI3K or phosphatase and tensin homolog deleted on chromosome 10 (PTEN) small interfering RNA (siRNA), will not differentiate the cellular mechanisms of their immune regulatory effects in vivo. In the current study, we used the Cre-LoxP system to create myeloid PTEN knockout (KO) mice to specifically study PI3K activation in myeloid cells in liver IRI. PTEN is a dual-specificity protein/lipid phosphatase, and it functions as a major negative regulator of the PI3K/Akt-signaling pathway. PTEN was originally identified as a tumor-suppressor gene, and loss of its function stimulates cell growth and survival (14). Its inhibition with small molecule inhibitor has been widely

*Division of Liver and Pancreas Transplantation, Department of Surgery, Dumont-UCLA Transplant Center, David Geffen School of Medicine at University of California-Los Angeles, Los Angeles, CA 90095; [†]Department of Liver Surgery, The First Affiliated Hospital of Nanjing Medical University, Nanjing, Jiansu Province, China 210029; and [‡]Department of Liver Surgery, Renji Hospital, Shanghai JiaoTong University School of Medicine, Shanghai, China 200127

[1]S.Y. and J.R. contributed equally to this work.

used in infarction models to ameliorate cardiomyocyte/neuron apoptosis and cell death (15–20). PTEN knockdown with its specific siRNA also was tested in a liver IR model recently (21, 22), with an implication of immune regulation. However, only correlative conclusions can be draw from these studies because of issues of target cell specificity, incomplete gene inhibition/downregulation, and off-target effects of chemical inhibitors and siRNAs. Our myeloid-specific KO model enabled us, for the first time to our knowledge, to determine specifically whether PTEN is directly involved in liver innate immune activation against IR.

Materials and Methods

Animals

PTEN-LoxP mice (generous gift from Dr. Hong Wu, University of California-Los Angeles, Los Angeles, CA) and the myeloid-specific Cre mice (Lyz2-Cre; The Jackson Laboratory, Bar Harbor, ME) were used to create myeloid-specific PTEN KO mice. Briefly, homozygous PTEN$^{loxP/loxP}$ mice were bred with homozygous Lyz2-Cre mice, and the heterozygous offspring (for both PTEN and Cre) were back-crossed with homozygous PTEN$^{loxP/loxP}$ mice. Mouse genotyping was performed by using a standard protocol with primers described in the JAX Genotyping protocols database. Animals were housed in the University of California-Los Angeles animal facility under specific pathogen–free conditions and received humane care according to the criteria outlined in the *Guide for the Care and Use of Laboratory Animals* prepared by the National Academy of Sciences and published by the National Institutes of Health.

Mouse liver IRI model

PTEN-normal and -deficient mice (6–8 wk old) were used in experiments. As described previously (23), mice anesthetized with sodium pentobarbital (60 mg/kg i.p.) were injected with heparin (100 mg/kg), and an atraumatic clip was used to interrupt the arterial and portal venous blood supply to the cephalad lobes of the liver. After 90 min of partial hepatic warm ischemia, the clip was removed, initiating hepatic reperfusion. Mice were sacrificed after 0, 6, or 24 h of reperfusion. Sham controls underwent the same procedure but without vascular occlusion. LPS (1 μg/mouse; LPS-EK; InvivoGen, San Diego, CA), anti–IL-10 (JES5-2A5), or control Ig (300 μg/mouse; both from Bio X Cell, West Lebanon, NH) was administered prior to the liver reperfusion via the portal vein. Other treatments include wortmannin (WM; 1 μg/g in 200 μl, i.p.; Tocris Bioscience) for 1 h and GdCl₃ (10 μg/g in 200 μl DMSO, i.p.; Sigma, St. Louis, MO) for 16 h prior to the onset of liver ischemia.

Serum alanine aminotransferase (sALT) levels were measured with an autoanalyzer by ANTECH Diagnostics (Los Angeles, CA). Part of the liver was fixed in 10% buffered formalin and embedded in paraffin. Liver sections (4 μM) were stained with H&E. The severity of liver IRI was graded blindly, on a scale from 0 to 4, using Suzuki's criteria. No necrosis, congestion/centrilobular ballooning is given a score of 0, whereas severe congestion and >60% lobular necrosis is given a score of 4 (24).

Liver macrophages and neutrophils were detected using primary rat anti-mouse F4/80 mAb (AbD Serotec, Raleigh, NC) and Ly6G mAb (BD Biosciences, San Jose, CA), respectively. The secondary, biotinylated goat anti-rat IgG was incubated with immunoperoxidase (ABC Kit; both from Vector, Burlingame, CA).

Myeloperoxidase assay

Liver myeloperoxidase (MPO) activities were measured. Briefly, the frozen tissue was thawed and placed in iced 0.5% hexadecyltrimethyl–ammonium bromide and 50 mM potassium phosphate buffer solution (pH 5). Each sample was homogenized and centrifuged at 15,000 rpm for 15 min at 4°C. Supernatants were mixed with H₂O₂–sodium acetate and tetramethyl-benzidine solutions. The change in absorbance was measured by spectrophotometry at 655 nm. One unit of MPO activity was defined as the quantity of enzyme degrading 1 μmol H₂O₂/min at 25°C/g of tissue.

Cell cultures

Cells were derived from PTEN-loxP$^{+/+}$ (Cre−ptenL/L) mice as PTEN normal/wild-type (WT) or from Lyz2-Cre$^{+/−}$ PTEN-loxP$^{+/+}$ (Cre+ptenL/L) mice as PTEN-deficient/KO after euthanasia (pentobarbital 100 mg/kg, i.p.).

Peritoneal macrophages were generated by injection of 1 ml 2% Bio-Gel P-100 (Bio-Rad, Hercules, CA) into the mouse peritoneal cavity, followed by peritoneal lavage with sterile PBS 4 d later.

Kupffer cells (KCs) were isolated as follows: livers were perfused in situ via the portal vein with calcium- and magnesium-free HBSS supplemented with 2% heat-inactivated FBS, followed by 0.27% collagenase IV (Sigma). Perfused livers were dissected and teased through 70-μm nylon mesh cell strainers (BD Biosciences). Nonparenchymal cells (NPCs) were separated from hepatocytes by centrifuging at 50 × g for 2 min three times. NPCs were suspended in HBSS and layered onto a 50%/25% two-step Percoll gradient (Sigma) in a 50-ml conical centrifuge tube and centrifuged at 1800 × g at 4°C for 15 min. KCs in the middle layer were collected and allowed to attach onto cell culture plates in DMEM with 10% FBS, 10 mM HEPES, 2 mM GlutaMax, 100 U/ml penicillin, and 100 μg/ml streptomycin for 15 min at 37°C. Nonadherent cells were removed by replacing the culture medium. The purity of KCs was 80% as assessed by immunofluorescence staining for F4/80.

Spleen macrophages were isolated using an immunomagnetic CD11b Positive Selection Kit (STEMCELL Technologies, Vancouver, BC, Canada), according to the manufacturer's manual.

Macrophages or KCs were cultured overnight prior to the start of stimulations with TLR ligands: 100 ng/ml LPS-EK, 1 μg/ml LAM-MS, or 1 μg/ml polyinosinic-polycytidylic acid (InvivoGen). Cells or culture supernatants were harvested after various lengths of stimulation for RNA, protein, and ELISA assays.

Quantitative RT-PCR

Total RNA (2 μg) was reverse-transcribed into cDNA using a SuperScript III First-Strand Synthesis System (Invitrogen, Carlsbad, CA). Quantitative PCR was performed using the DNA Engine with Chromo 4 Detector (MJ Research, Waltham, MA). In a final reaction volume of 20 μl, the following were added: 1× SuperMix (Platinum SYBR Green qPCR Kit, Invitrogen), cDNA, and 0.5 mM of each primer. Amplification conditions were 50°C for 2 min and 95°C for 5 min, followed by 50 cycles of 95°C (15 s) and then 60°C for 30 s. Primers used to amplify specific mouse gene fragments were the same as described previously (25).

Western blots

Tissue or cellular proteins were extracted with ice-cold lysis buffer (1% Triton X-100, 0.5% sodium deoxycholate, 0.1% SDS, 10% glycerol, 137 mM sodium chloride, 20 mM Tris [pH 7.4]). Proteins (20 μg) were subjected to 12% SDS-PAGE and transferred to polyvinylidene difluoride nitrocellulose membrane. Abs against PTEN, p-AKT, Stat3, foxo1, β-actin (Cell Signaling Technology, San Diego, CA), and HO-1 (Stressgen Biotech, Victoria, BC, Canada) were used for Western blot analysis.

ELISA

Cytokine (TNF-α, IL-6, IL-12p40, and IL-10) secretion in cell culture supernatants or serum was measured by ELISA, according to the manufacturer's protocol (eBioscience, San Diego, CA).

Statistical analysis

Results are shown as mean ± SD. Statistical analyses were performed using the unpaired Student t test, with $p < 0.05$ (two-tailed) considered significant.

Results

Myeloid PTEN deficiency protects livers from IRI

Three PTEN mice, including PTEN-loxP$^{+/+}$ (Cre−ptenL/L), Lyz2-Cre$^{+/−}$ PTEN-loxP$^{+/−}$ (Cre+ptenL/−), and Lyz2-Cre$^{+/−}$ PTEN-loxP$^{+/+}$ (Cre+ptenL/L), which had normal, haploid-deficient, or completely deficient PTEN in myeloid cells, respectively, as documented by Western blots of PTEN of peritoneal macrophages (Fig. 1A, *upper panel*), were used in our liver IRI experiments. Although total liver tissue levels of PTEN were similar between WT and myeloid PTEN KO mice, selective PTEN deficiency in liver NPC versus parenchymal cell populations was confirmed (Fig. 1A, *lower panels*). Unlike its tumor-suppressor function, myeloid PTEN regulated the development of liver IRI in a haploid-sufficient manner. Only complete PTEN deficiency, and not haploid PTEN deficiency, protected mice from liver IRI, as shown by lower sALT levels and better-preserved liver architecture (H&E staining), with lower Suzuki scores, at both 6 and 24 h of reperfusion in Cre+ptenL/L, but not Cre+ptenL/− or Cre−ptenL/L,
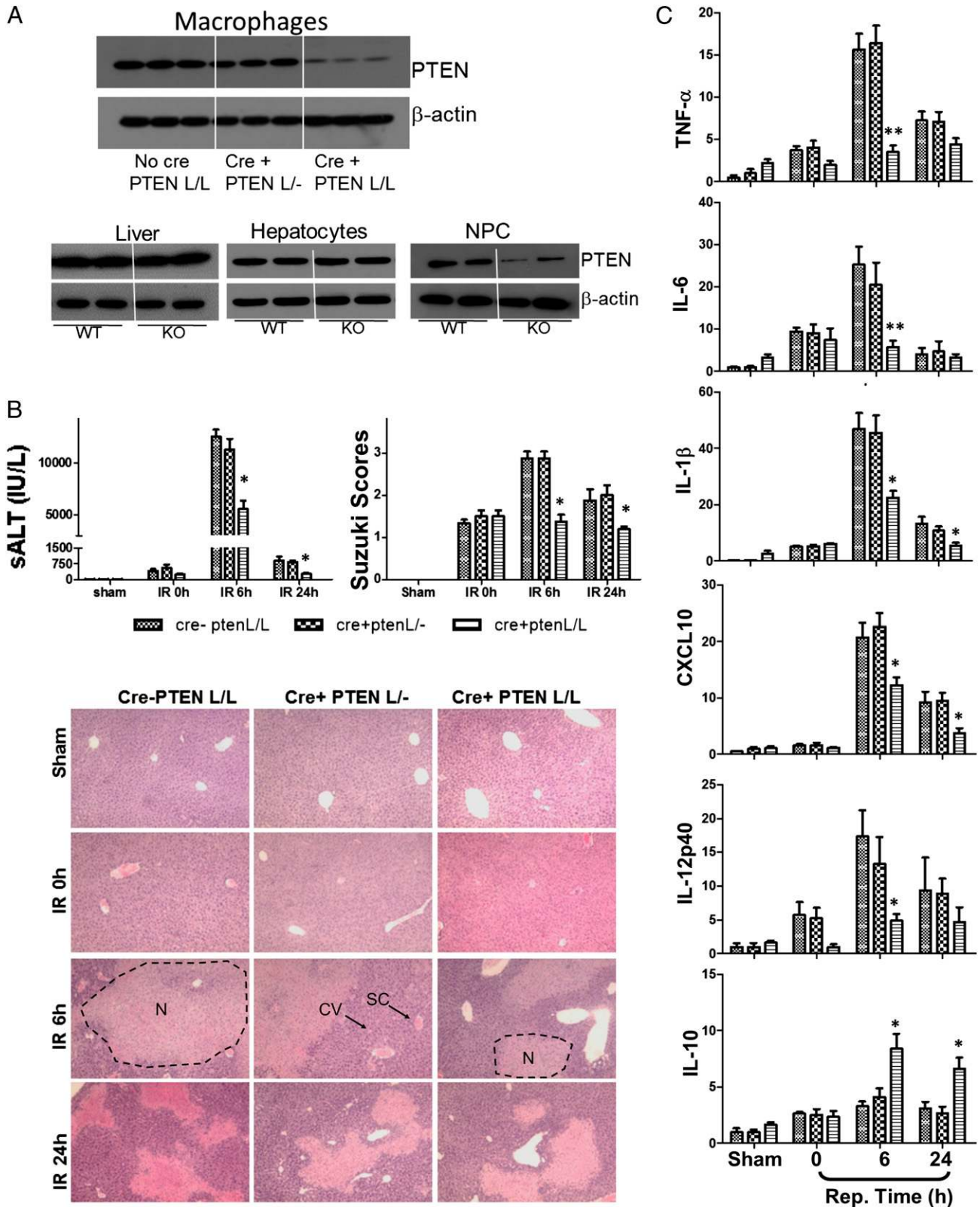
FIGURE 1. Complete myeloid PTEN KO protected livers from IRI. PTEN-loxP$^{+/+}$ (Cre-PTEN L/L), Lyz-Cre$^{+/-}$ PTEN-loxP$^{+/-}$ (Cre+PTEN L/−), and Lyz-Cre$^{+/-}$ PTEN-loxP$^{+/+}$ (Cre+PTEN L/L) mice were used in liver IR experiments, as described in *Materials and Methods*. (**A**) Western blots of PTEN in peritoneal macrophages, as well as in liver tissues, hepatocytes, and NPCs, isolated from WT or myeloid PTEN KO mice. (**B**) sALT and Suzuki scores of liver histological analysis (H&E stain, original magnification ×40) in different groups of mice subjected to either sham operation or 90 min of ischemia, followed by 0, 6 or 24 h of reperfusion. Typical areas with sinusoidal congestion (SC), cytoplasmic vacuolization (CV) and hepatocellular necrosis (N) are indicated. (**C**) Quantitative RT-PCR analysis of inflammatory gene expression in sham-operated and ischemic livers after 0, 6, or 24 h of reperfusion. The ratios of target gene/HPRT were plotted against different experimental groups. Bar labels are the same as in (B). Representative results of two different experiments ($n = 3$–4/group). *$p < 0.05$, **$p < 0.01$.

mice (Fig. 1B). Indeed, IR livers in PTEN KO mice exhibited less edema, minimal sinusoidal congestion and cytoplasmic vacuolization, and decreased hepatocellular necrosis compared with control animals. The liver proinflammatory immune response against IR was also regulated similarly by myeloid PTEN, as shown by lower induction of proinflammatory genes, including TNF-α, IL-6, IL-1B, CXCL10, and IL-12p40, and higher induction of anti-inflammatory IL-10 genes only in livers of complete, but not haploid, PTEN KO mice (Fig. 1C).

Because PTEN is a tumor-suppressor gene and regulates cell proliferation, we compared myeloid cell compositions between WT and myeloid PTEN KO mice. Increased numbers of monocytes and neutrophils were found in peripheral blood (data not shown) and livers (F4/80+ or Ly6G+ cells in sham) of KO animals compared with WT controls. However, their inflammatory infiltration into livers in response to IR was diminished. In sharp contrast to the significant increases in PTEN-normal cells, PTEN-deficient F4/80+ cells were not increased (or showed decreased trend) in IR livers at 6 h postreperfusion; PTEN-deficient Ly6G+ cells were increased to a significantly lower degree in IR livers than in normal cells at both 6 and 24 h postreperfusion (Fig. 2A, 2B). Liver MPO activities also were reduced in livers of KO mice at both 6 and 24 h of reperfusion (Fig. 2C). Thus, myeloid PTEN deficiency protected livers from IRI. This might be due to impairment of myeloid cell function rather than cell depletion in KO mice.

PI3K activation–dependent IL-10 induction is responsible for liver protection in myeloid PTEN KO mice

Because PTEN could function via both PI3K-dependent and -independent pathways, we determined whether the liver protection from IR in myeloid PTEN-deficient mice was dependent on PI3K activation using a PI3K inhibitor (WM). Indeed, injections of the inhibitor restored liver IRI in KO mice, as evidenced by increased sALT levels and more severely damaged liver histological architecture (H&E staining), with higher Suzuki scores (Fig. 3A). No significant increases in liver IRI were observed in WT mice treated with WM (data not shown), as we reported previously (11).
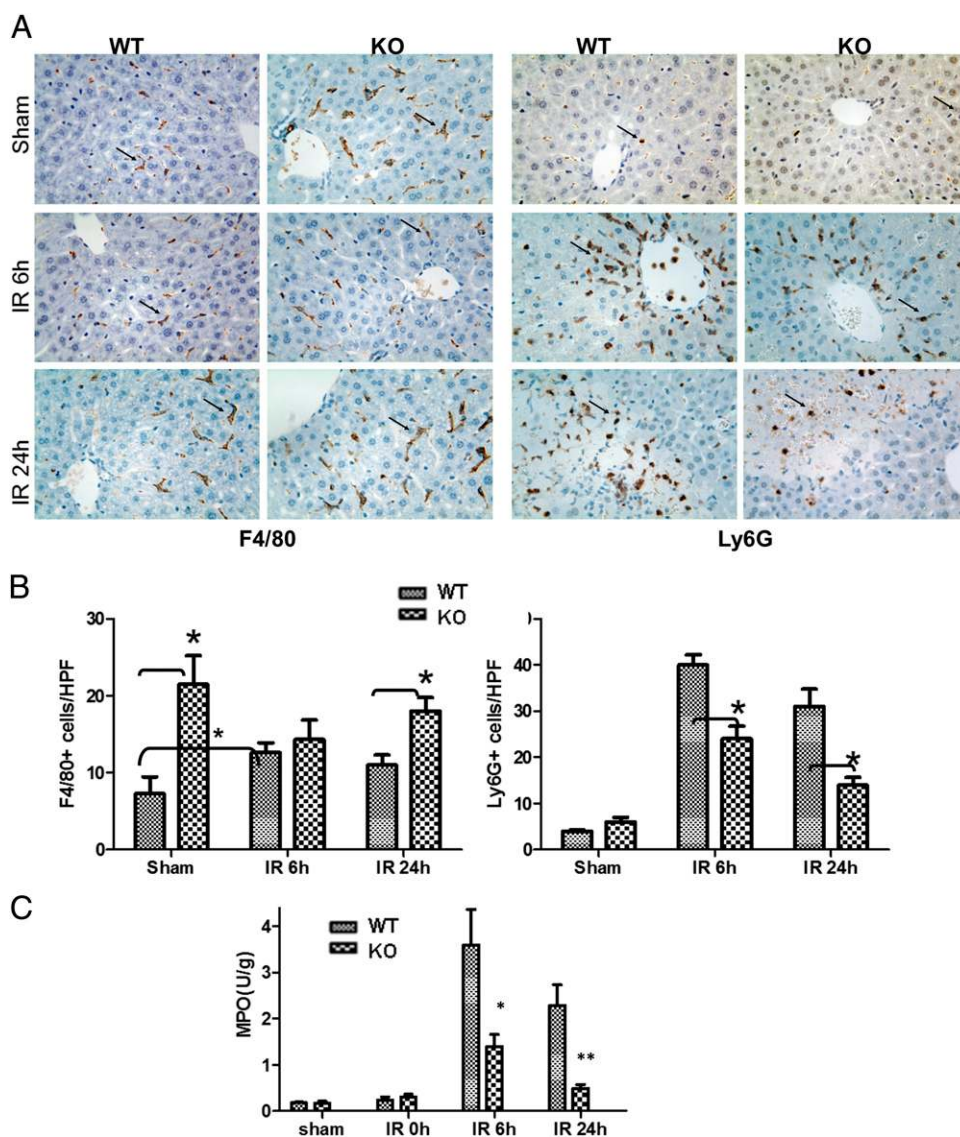
FIGURE 2. Myeloid PTEN KO diminished liver myeloid cell infiltration and activation in IR. Sham and ischemic liver tissues from PTEN-loxP+/+ (WT) and Lyz-Cre+/− PTEN-loxP+/+ (KO) mice were harvested after 6 or 24 h of reperfusion. (**A**) Macrophage and neutrophil infiltration was analyzed by immunohistological staining with Abs against F4/80 and Ly6G, respectively (original magnification ×40), in sham and IR livers at 6 and 24 h post-reperfusion. Arrows indicate positive cells. (**B**) F4/80+ or Ly6G+ cells were quantitated by counting numbers of positive cells/area. (**C**) MPO activity was measured in these liver tissues. Representative results of two different experiments (n = 3–4/group). *p < 0.05, **p < 0.01.
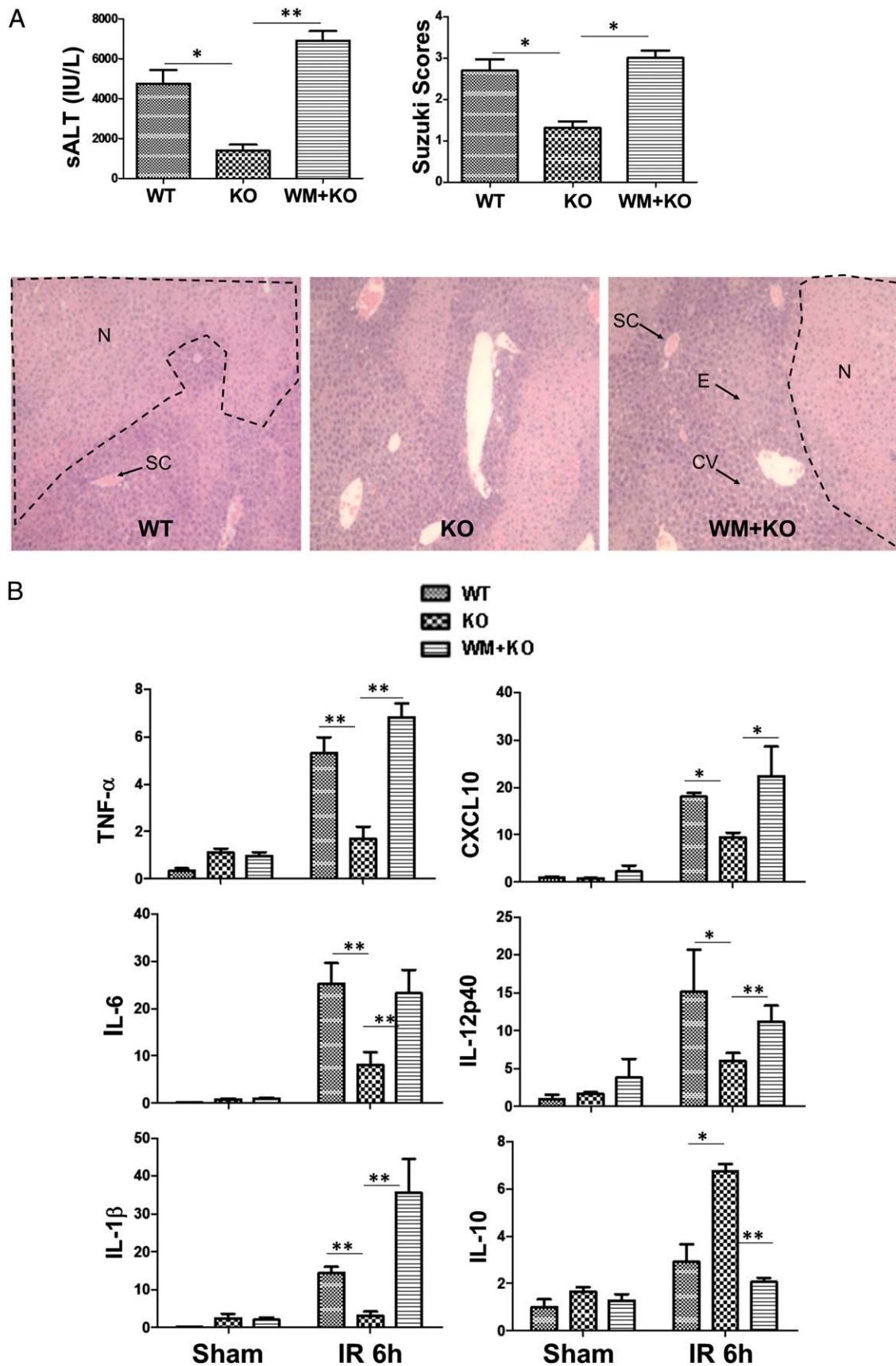
FIGURE 3. PI3K activation protects livers from IRI in myeloid PTEN KO mice. PTEN-loxP^{+/+} (WT) and Lyz-Cre^{+/−} PTEN-loxP^{+/+} (KO) mice were used in our liver IR experiment, as described in *Materials and Methods*. A separate group of KO mice treated with PI3K inhibitor (WM) prior to the start of liver ischemia was included. (**A**) Liver IRI was evaluated at 6 h postreperfusion by measuring sALT and assessing liver histology (H&E stain, original magnification ×40) using Suzuki scores. Typical areas with edema (E), sinusoidal congestion (SC), cytoplasmic vacuolization (CV), and hepatocellular necrosis (N) are indicated. (**B**) Liver immune response against IR was determined by quantitative RT-PCR analysis of inflammatory   (*Figure legend continues*)
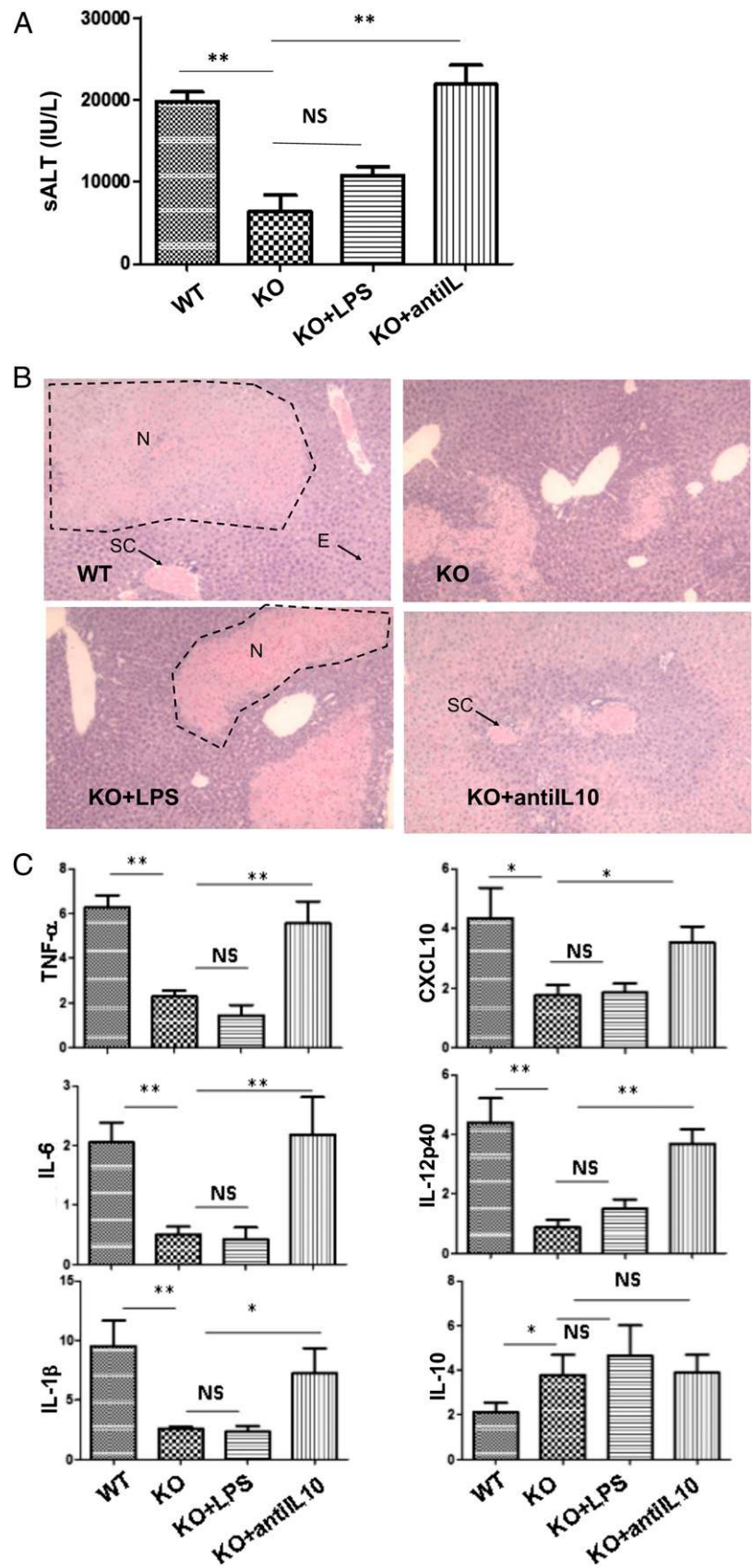
FIGURE 4. Myeloid PTEN KO protected livers against IRI via an IL-10–dependent mechanism. Anti–IL-10 Abs or LPS were administered to KO mice after liver ischemia and prior to the start of reperfusion via the portal vein, as described in *Materials and Methods*. WT and KO mice without any treatment were included as controls. Liver IRI was evaluated at 6 h postreperfusion by measuring sALT (**A**) and assessing liver histology (H&E stain, original magnification ×40) (**B**). Typical areas with edema (E), sinusoidal congestion (SC), and hepatocellular necrosis (N) are indicated. (**C**) Liver immune response against IR was determined by quantitative RT-PCR analysis of inflammatory gene expressions in IR livers. The ratios of target gene/housekeeping gene (HPRT) expression levels were plotted for different experimental groups. Representative results of two different experiments (*n* = 3–4/group). *$p < 0.05$, **$p < 0.01$.

gene expression in sham-operated and IR livers. The ratios of target gene/housekeeping gene HPRT expression levels were plotted for different experimental groups. Representative results of two different experiments (*n* = 3–4/group). *$p < 0.05$, **$p < 0.01$.

In addition, liver proinflammatory immune response against IR was recreated that intrahepatic TNF-α, IL-1B, IL-6, IL-12p40, and CXCL10 transcription levels were increased, whereas IL-10 was decreased in the inhibitor-treated myeloid PTEN KO mice (Fig. 3B). Thus, PI3K activation was critical for liver regulatory immune response and protection from IRI in myeloid PTEN-deficient mice.

To test the functional significance of IL-10 in liver protection by myeloid PTEN deficiency, we administered anti–IL-10 Abs prior to the start of liver ischemia. In addition, LPS was injected into a separate group of KO mice to determine whether the lack of TLR activation played a role in the defective inflammatory immune response to IR in PTEN-deficient mice. Liver injury and immune responses were measured at 6 h postreperfusion. Our results clearly showed that anti–IL-10, but not LPS, restored liver IRI and proinflammatory immune activation. Treatment with anti–IL-10, but not LPS, resulted in significant increases in sALT levels and worsening of liver histopathology (H&E staining), with higher Suzuki scores, in PTEN KO mice (Fig. 4A, 4B). Liver cytokine/chemokine induction, including TNF-α, IL-6, IL-1B, IL-14p40, and CXCL10, as measured by quantitative RT-PCR, also was in-

creased in the same group of treated KO mice (Fig. 4C). The IL-10 gene induction was not changed much by the treatment. Thus, myeloid PTEN deficiency protected livers from IRI via an IL-10–mediated immune-regulatory mechanism.

PTEN regulates macrophage differentiation

Because KCs are the major responding cells in liver innate immune activation by IR, we determined whether myeloid PTEN KO affected their functions. KCs and splenic macrophages were isolated from livers of both control and KO mice and stimulated in vitro with LPS. ELISA results showed that PTEN KO KCs and spleen macrophages produced significantly less TNF-α and more IL-10 in response to TLR stimulation compared with those from WT controls (Fig. 5A).

Macrophages can be differentiated into two distinctive types, classical proinflammatory M1 or alternative immune regulatory M2. To determine whether PTEN KO resulted in the development of M2 macrophages, we measured the expression of macrophage differentiation markers in KCs and peritoneal macrophages by quantitative RT-PCR. Clearly, PTEN KO cells expressed constitutively higher levels of Arg1 and Mrc1 but lower levels of Nos2

FIGURE 5. PTEN deficiency results in M2 macrophage development. (**A**) Cytokine production by KCs and splenic macrophages from WT and myeloid PTEN KO mice. Liver and spleen macrophages were isolated from either WT or KO mice, as described in *Materials and Methods*, and cultured in vitro with or without LPS stimulation for 24 h. TNF-α and IL-10 levels in culture supernatants were measured by ELISA. (**B**) Peritoneal macrophages were isolated from WT and PTEN KO mice, and M1/M2 marker gene expression was measured by quantitative RT-PCR. Note, left y-axis corresponds to Arg; right y-axis corresponds to Mrc and Nos2. (**C**) Inflammatory cytokine/chemokine production by peritoneal macrophages. Cells were cultured in vitro for 24 h before TLR stimulation. Cytokines in culture supernatants after 24 h of stimulation were measured by ELISA. Representative results of two different experiments (n = 3/group). *p < 0.05, **p < 0.01.
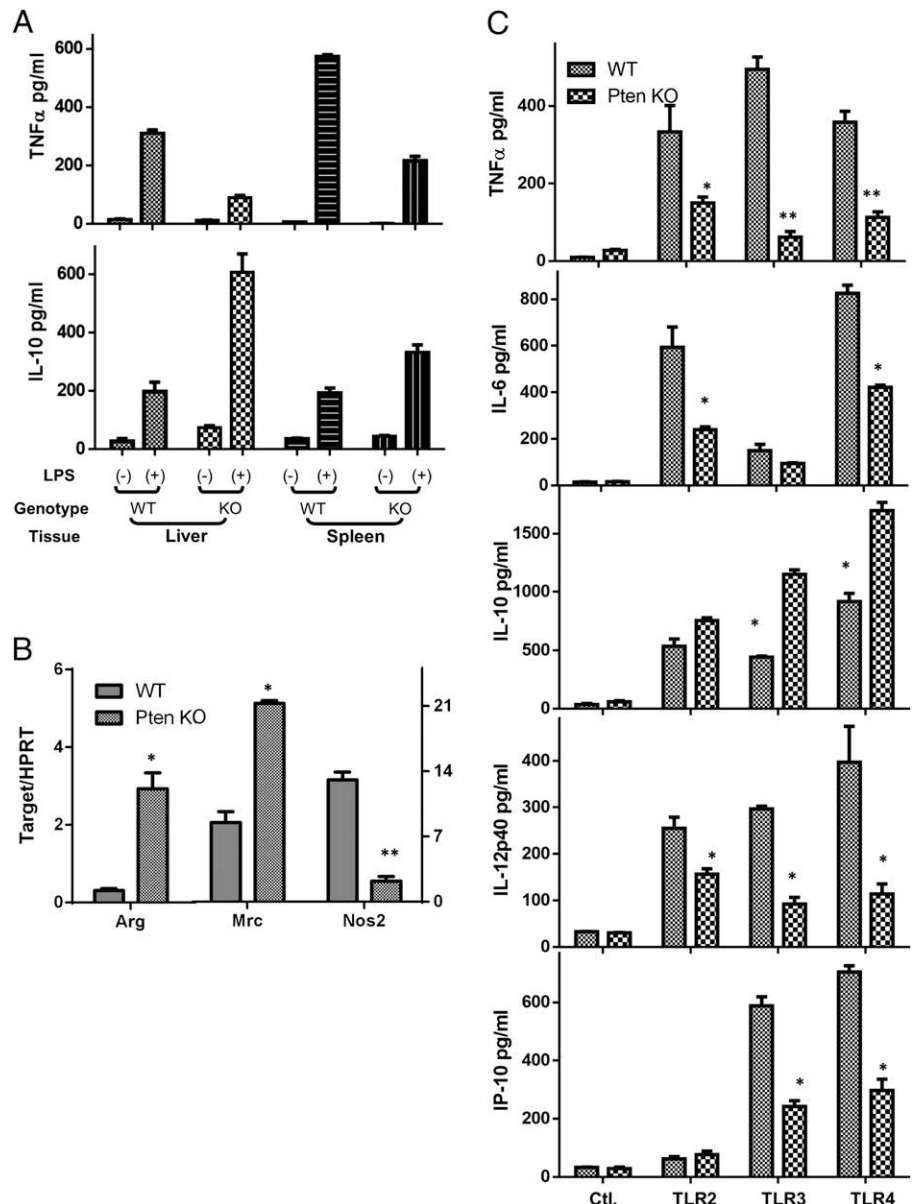
gene (Fig. 5B). Functionally, these KO macrophages produced significantly less TNF-α, IL-6, IL-12p40, and CXCL10, but more IL-10, than did WT cells in response to LPS (Fig. 5C). Additionally, their responses to other TLR ligands also became less proinflammatory: less TNF-α and IL-6 against the TLR2 ligand and less TNF-α, IL-12p40, and CXCL10, but more IL-10, against the TLR3 ligand (Fig. 5C). Furthermore, Western blot results showed that these KO cells responded to LPS stimulation with reduced activation (phosphorylation) of Stat1 but enhanced activation of Stat3 and Stat 6 (Fig. 6). Consistent with its role in limiting PI3K activation, PTEN KO resulted in its constitutive activation, because Akt was phosphorylated at both S473 and T308 prior to TLR stimulation. Akt phosphorylation was further increased after stimulation (Fig. 6). Thus, PTEN regulates macrophage differentiation, and its deficiency results in the development of M2 macrophages.

PTEN-deficient KCs protect livers against IRI

To test potential immune-regulatory functions of PTEN KO macrophages in vivo in response to IR, GdCl$_3$ was used to inactivate these cells prior to the start of liver ischemia. Consistent with previous reports, GdCl$_3$-treated WT mice had decreased levels of sALT with better preserved liver architecture (H&E staining) (Fig. 7A, 7B). Liver inflammatory gene induction, including TNF-α, IL-1B, IL-6, IL-12B, CXCL10, and IL-10, also were decreased compared with their vehicle-treated controls (Fig. 7C). In contrast, GdCl$_3$-treated KO mice had increased levels of sALT and liver proinflammatory gene expression compared with their controls. However, the IL-10 gene level was downregulated by the treatment in KO mice. Thus, unlike its protective effect in WT mice, GdCl$_3$ treatment resulted in increased liver IRI and enhanced tissue proinflammatory immune activation in myeloid PTEN KO mice, indicating that PTEN KO macrophages exerted anti-inflammatory functions in vivo in the pathogenesis of liver IRI.
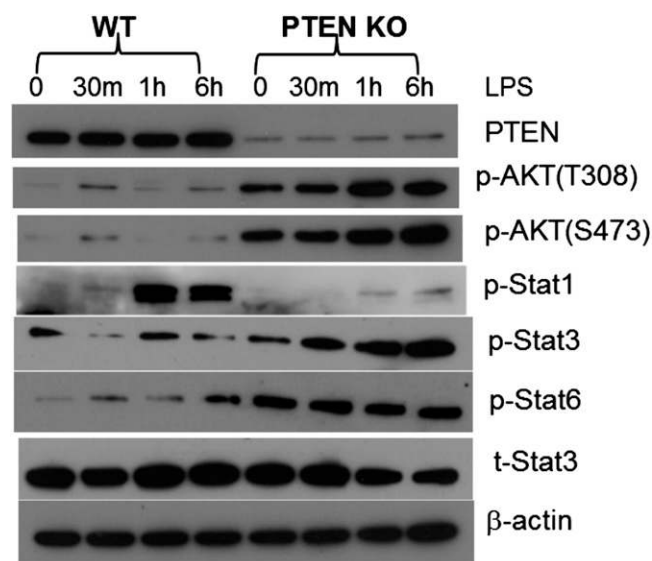
Discussion

Our current study provides strong evidence that PTEN is involved directly in liver innate immune response against IR by regulating

FIGURE 6. Macrophage intracellular signaling-pathway activation. Peritoneal macrophages were not stimulated (0) or were stimulated with LPS for 30 min or 1 or 6 h, and cell lysates were prepared and analyzed by Western blotting to determine intracellular signaling molecule activation (phosphorylation). Representative results of two different experiments.

macrophage differentiation and activation. Myeloid PTEN deficiency results in the development of M2-type macrophages, which respond to IR-induced innate immune stimulation by producing a regulatory inflammatory response with higher levels of IL-10, but lower levels of TNF-α, IL-6, and CXCL10, which protects livers from IRI. These findings establish an innate immune regulatory role for PTEN in vivo in a relevant clinical disease model and provide the rationale for selectively targeting this signaling pathway as a novel therapeutic strategy to ameliorate tissue inflammatory diseases.

Myeloid PTEN-deficient mice have been used to study roles of PTEN in the innate immune response. In vitro, PTEN was shown to negatively regulate FcγR signaling, but positively regulate TLR4 signaling, in that TNF-α production was increased in response to FcγR stimulation but decreased against LPS in PTEN KO macrophages compared with WT controls (26). These PTEN KO macrophages also showed enhanced phagocytic ability. In a murine pneumococcal pneumonia model, myeloid PTEN deficiency dampened pulmonary inflammation, reduced neutrophil infiltration, and augmented phagocytosis, which led to decreased tissue injury and improved survival (27). Studies of neutrophils, the other type of myeloid cells, revealed that PTEN suppressed neutrophil chemotaxis both in vitro and in vivo (28–30). In a neutropenia-associated pneumonia model, PTEN-deficient neutrophils, as well as macrophages, accumulated more in inflamed lungs, which resulted in increased production of proinflammatory cytokines and chemokines (29); this is very different from our finding in a liver inflammatory injury model. Thus, the way in which myeloid PTEN regulates immune responses can vary drastically, probably because of differences in the cellular and molecular mechanisms of disease pathogenesis.

Our results show that IR-induced liver inflammation was alleviated in myeloid PTEN KO mice. Despite the fact that both macrophages and neutrophils cells were present at higher levels in sham livers of these KO animals, they failed to respond to IR. Liver macrophages are the major responding cells to IR and are responsible for triggering tissue inflammation, leading to neutrophil activation and infiltration. Inhibition of the macrophage proinflammatory response by PTEN KO would result in diminished neutrophil infiltration/activation. In fact, we found that PTEN KO macrophages became the anti-inflammatory M2 type, which actively secrete IL-10 in response to innate TLR stimulation. Thus, neutrophils might have been inactivated by the regulatory immune response generated by PTEN KO macrophages. This was supported by our finding that both GdCl3, which inactivates KCs/macrophages, and anti–IL-10 Abs reversed the nature of the liver immune response and recreated IRI in myeloid PTEN KO mice. In both cases, local innate immune cells, DCs and neutrophils, were free from the KC/IL-10–mediated immune regulation and became activated in response to IR.

As the key negative regulator of the prosurvival PI3K/Akt signaling pathways, PTEN has been studied extensively in brain and myocardial IRI models. A transient PTEN downregulation was identified as a physiological response to ischemia in these tissues. Posttranslational modifications of PTEN, including proteolytic degradation, phosphorylation, and ubiquitination-mediated nuclear relocation, were responsible for the reduction of its lipid phosphatase activities, which correlated with PI3K activation (15, 31, 32). PI3K/Akt activation has been closely associated with ischemia preconditioning, which represents one the most effective protective procedures against IRI. Thus, pharmacological inhibitors of PTEN, such as bisperoxovanadium (bpv), may functionally simulate ischemia preconditioning. Indeed, multiple studies showed that PTEN inhibition protected brains/hearts from stroke/
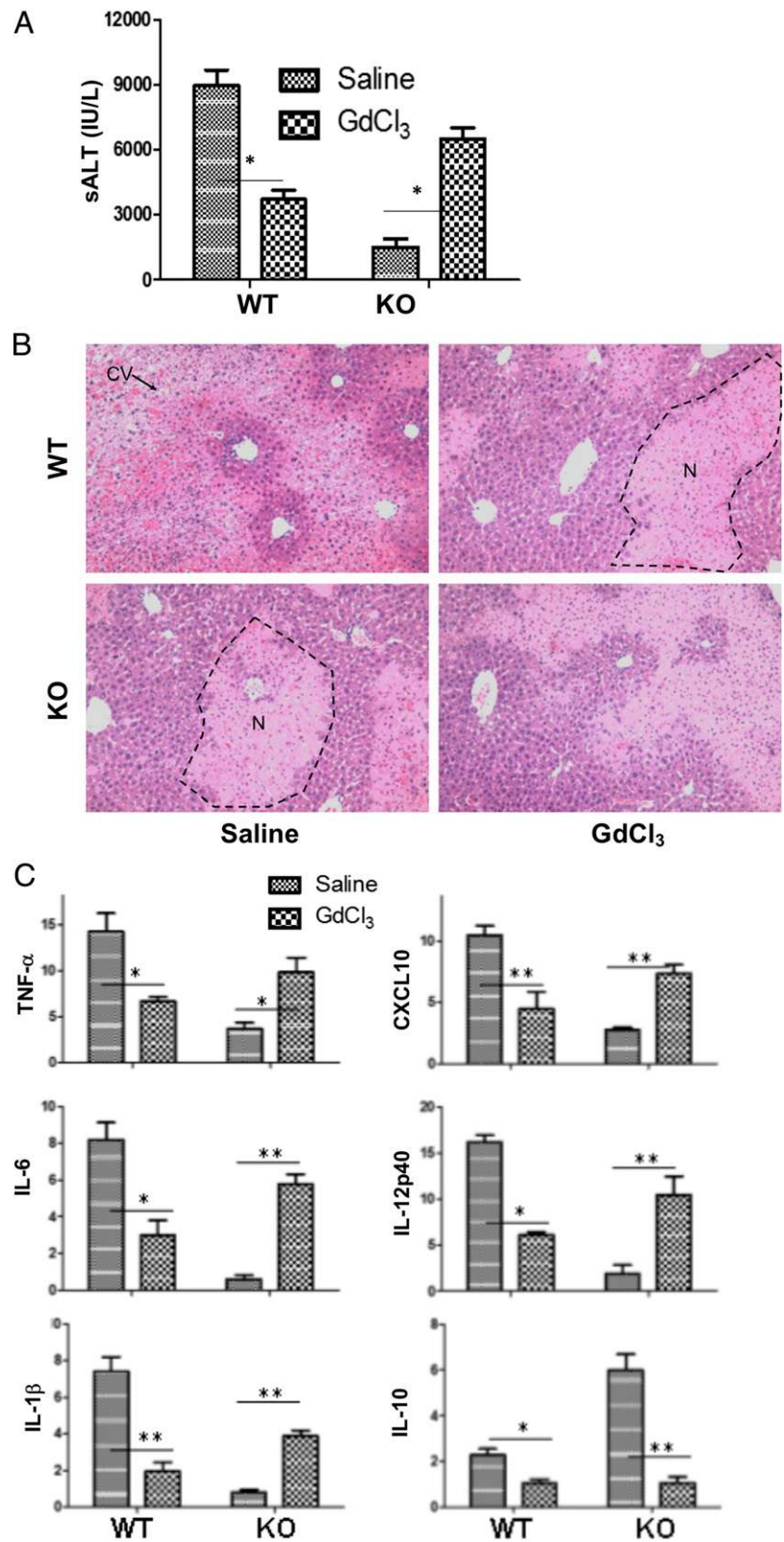
FIGURE 7. PTEN KO macrophages protect livers from IRI. Saline or GdCl₃ were administered 24 h prior to the start of liver ischemia, as described in *Materials and Methods*. Liver IRI was evaluated at 6 h postreperfusion by measuring sALT (**A**) and assessing liver histology (H/E stain, original magnification ×40) (**B**). Typical areas with cytoplasmic vacuolization (CV), and hepatocellular necrosis (N) are indicated. (**C**) Liver immune response against IR was determined by quantitative RT-PCR analysis of inflammatory gene expression in IR livers. The ratios of target gene/housekeeping gene (HPRT) expression levels were plotted for different experimental groups. Representative results of two different experiments ($n = 3$–4/group). *$p < 0.05$, **$p < 0.01$.

infarction (16, 18, 20, 33–35). Inhibition of caspase 3 activation and promotion of mTOR activation have been associated with the beneficial effect of bpv (16, 36). In vitro, PI3K activation was critical for hepatocyte preconditioning against hypoxia/reperfusion (37), which could be mimicked by bpv and translated into in vivo protection against liver IRI (38). More recently, studies using siRNA to knockdown PTEN were shown to promote Akt/β-catenin/Foxo1 signaling in livers, leading to local enhancement of anti-apoptotic gene induction (21). Although a liver inflammatory immune response was also reduced, it might not be a direct effect in liver innate immune cells, but rather an indirect one by reducing damage-associated molecular pattern release from necrotic parenchymal cells, which are protected from IR-induced cell death by PTEN inhibition/downregulation. Interestingly, we observed that myeloid PTEN deficiency does not impact liver total PTEN levels; only complete PTEN KO in macrophages showed significant

immune regulatory effect. These indicate that hepatocyte PTEN is dominant quantitatively in the liver. Only cell-specific genetic approaches would allow us to dissect PTEN functions in liver innate immune cells without interference from hepatocytes. Thus, to our knowledge, our study is the first to document immune regulatory function of PTEN in a tissue IR model.

PTEN regulates the liver immune response against IR in a "haploid sufficient" manner: significant effects were observed only in total myeloid PTEN-deficient animals. This is in sharp contrast to the haploid-insufficient property in its tumor suppressor function in that loss of heterozygosity or partial inhibition of its expression/activity is sufficient to promote carcinogenesis. Hepatocyte-specific PTEN KO induces hepatomegaly, hepatocellular adenoma, and hepatocellular carcinoma with aging and promotes the development of steatohepatitis and fibrosis (39, 40). In our myeloid PTEN-deficient mice, the numbers of both neutrophils and monocytes were increased in peripheral blood and liver tissues, consistent with the role of PTEN in cell proliferation. However, the functions of these cells were altered. Tissue macrophages from both liver and spleen, as well as those from peritoneum, were defective in terms of their proinflammatory immune activation by TLR ligands. DCs from the same animals, which are PTEN normal, remain capable of mounting similar innate immune responses as do those from WT animals (data not shown). This is supported by the result from our in vivo KC-depletion experiment, in which liver inflammation and injury were recreated in PTEN KO mice after GdCl$_3$ treatment.

Because PTEN negatively regulates PI3K activation, its deficiency results in the constitutive activation of this kinase pathway, as documented by higher levels of Akt phosphorylation. Our result showed that PI3K activation was critical for the liver protection phenotype in PTEN KO mice, which actually facilitated the differentiation of M2-type macrophages. M2 macrophages were shown to protect kidneys, brain, and hindlimbs from ischemia injuries (41–43) by promoting either the resolution of tissue inflammation or healing/recovery. Our study extended the role of M2 macrophages in liver IRI. Mechanistically, the PI3K/Akt/mTOR pathway was shown to regulate macrophage differentiation (44, 45), in part via miR-155 upregulation. The molecular details of the M2-differentiation program in PTEN KO cells remain to be determined.

In summary, our data document an innate immune-regulatory role for PTEN in the liver inflammatory response against IR. Its genetic inactivation in macrophages results in their differentiation into the anti-inflammatory M2 type, which protects livers from IRI via an IL-10–dependent mechanism.

Disclosures

The authors have no financial conflicts of interest.

References

1. Fiorini, R. N., S. F. Shafizadeh, C. Polito, D. W. Rodwell, G. Cheng, Z. Evans, C. Wan, S. Belden, J. K. Haines, J. Birsner, et al. 2004. Anti-endotoxin monoclonal antibodies are protective against hepatic ischemia/reperfusion injury in steatotic mice. *Am. J. Transplant.* 4: 1567–1573.
2. Tsung, A., R. Sahai, H. Tanaka, A. Nakao, M. P. Fink, M. T. Lotze, H. Yang, J. Li, K. J. Tracey, D. A. Geller, and T. R. Billiar. 2005. The nuclear factor HMGB1 mediates hepatic injury after murine liver ischemia-reperfusion. *J. Exp. Med.* 201: 1135–1143.
3. Zhai, Y., X. D. Shen, R. O'Connell, F. Gao, C. Lassman, R. W. Busuttil, G. Cheng, and J. W. Kupiec-Weglinski. 2004. Cutting edge: TLR4 activation mediates liver ischemia/reperfusion inflammatory response via IFN regulatory factor 3-dependent MyD88-independent pathway. *J. Immunol.* 173: 7115–7119.
4. Takeda, K., T. Kaisho, and S. Akira. 2003. Toll-like receptors. *Annu. Rev. Immunol.* 21: 335–376.
5. Akira, S., and K. Takeda. 2004. Toll-like receptor signalling. *Nat. Rev. Immunol.* 4: 499–511.
6. Fukao, T., and S. Koyasu. 2003. PI3K and negative regulation of TLR signaling. *Trends Immunol.* 24: 358–363.
7. Fukao, T., M. Tanabe, Y. Terauchi, T. Ota, S. Matsuda, T. Asano, T. Kadowaki, T. Takeuchi, and S. Koyasu. 2002. PI3K-mediated negative feedback regulation of IL-12 production in DCs. *Nat. Immunol.* 3: 875–881.
8. Martin, M., K. Rehani, R. S. Jope, and S. M. Michalek. 2005. Toll-like receptor-mediated cytokine production is differentially regulated by glycogen synthase kinase 3. *Nat. Immunol.* 6: 777–784.
9. Beurel, E., S. M. Michalek, and R. S. Jope. 2010. Innate and adaptive immune responses regulated by glycogen synthase kinase-3 (GSK3). *Trends Immunol.* 31: 24–31.
10. Ohtani, M., S. Nagai, S. Kondo, S. Mizuno, K. Nakamura, M. Tanabe, T. Takeuchi, S. Matsuda, and S. Koyasu. 2008. Mammalian target of rapamycin and glycogen synthase kinase 3 differentially regulate lipopolysaccharide-induced interleukin-12 production in dendritic cells. *Blood* 112: 635–643.
11. Ren, F., Z. Duan, Q. Cheng, X. Shen, F. Gao, L. Bai, J. Liu, R. W. Busuttil, J. W. Kupiec-Weglinski, and Y. Zhai. 2011. Inhibition of glycogen synthase kinase 3 beta ameliorates liver ischemia reperfusion injury by way of an interleukin-10-mediated immune regulatory mechanism. *Hepatology* 54: 687–696.
12. Hers, I., E. E. Vincent, and J. M. Tavaré. 2011. Akt signalling in health and disease. *Cell. Signal.* 23: 1515–1527.
13. Hemmings, B. A., and D. F. Restuccia. 2012. PI3K-PKB/Akt pathway. *Cold Spring Harb. Perspect. Biol.* 4: a011189.
14. Song, M. S., L. Salmena, and P. P. Pandolfi. 2012. The functions and regulation of the PTEN tumour suppressor. *Nat. Rev. Mol. Cell Biol.* 13: 283–296.
15. Cai, Z., and G. L. Semenza. 2005. PTEN activity is modulated during ischemia and reperfusion: involvement in the induction and decay of preconditioning. *Circ. Res.* 97: 1351–1359.
16. Keyes, K. T., J. Xu, B. Long, C. Zhang, Z. Hu, and Y. Ye. 2010. Pharmacological inhibition of PTEN limits myocardial infarct size and improves left ventricular function postinfarction. *Am. J. Physiol. Heart Circ. Physiol.* 298: H1198–H1208.
17. Li, D., Y. Qu, M. Mao, X. Zhang, J. Li, D. Ferriero, and D. Mu. 2009. Involvement of the PTEN-AKT-FOXO3a pathway in neuronal apoptosis in developing rat brain after hypoxia-ischemia. *J. Cereb. Blood Flow Metab.* 29: 1903–1913.
18. Mao, L., J. Jia, X. Zhou, Y. Xiao, Y. Wang, X. Mao, X. Zhen, Y. Guan, N. J. Alkayed, and J. Cheng. 2013. Delayed administration of a PTEN inhibitor BPV improves functional recovery after experimental stroke. *Neuroscience* 231: 272–281.
19. Siddall, H. K., C. E. Warrell, D. M. Yellon, and M. M. Mocanu. 2008. Ischemia-reperfusion injury and cardioprotection: investigating PTEN, the phosphatase that negatively regulates PI3K, using a congenital model of PTEN haploinsufficiency. *Basic Res. Cardiol.* 103: 560–568.
20. Zhao, J., Y. Qu, J. Wu, M. Cao, D. M. Ferriero, L. Zhang, and D. Mu. 2013. PTEN inhibition prevents rat cortical neuron injury after hypoxia-ischemia. *Neuroscience* 238: 242–251.
21. Kamo, N., B. Ke, R. W. Busuttil, and J. W. Kupiec-Weglinski. 2013. PTEN-mediated Akt/β-catenin/Foxo1 signaling regulates innate immune responses in mouse liver ischemia/reperfusion injury. *Hepatology* 57: 289–298.
22. Ke, B., X. D. Shen, H. Ji, N. Kamo, F. Gao, M. C. Freitas, R. W. Busuttil, and J. W. Kupiec-Weglinski. 2012. HO-1-STAT3 axis in mouse liver ischemia/reperfusion injury: regulation of TLR4 innate responses through PI3K/PTEN signaling. *J. Hepatol.* 56: 359–366.
23. Shen, X. D., B. Ke, Y. Zhai, F. Amersi, F. Gao, D. M. Anselmo, R. W. Busuttil, and J. W. Kupiec-Weglinski. 2002. CD154-CD40 T-cell costimulation pathway is required in the mechanism of hepatic ischemia/reperfusion injury, and its blockade facilitates and depends on heme oxygenase-1 mediated cytoprotection. *Transplantation* 74: 315–319.
24. Suzuki, S., L. H. Toledo-Pereyra, F. J. Rodriguez, and D. Cejalvo. 1993. Neutrophil infiltration as an important factor in liver ischemia and reperfusion injury. Modulating effects of FK506 and cyclosporine. *Transplantation* 55: 1265–1272.
25. Zhai, Y., X. D. Shen, F. Gao, A. Zhao, M. C. Freitas, C. Lassman, A. D. Luster, R. W. Busuttil, and J. W. Kupiec-Weglinski. 2008. CXCL10 regulates liver innate immune response against ischemia and reperfusion injury. *Hepatology* 47: 207–214.
26. Cao, X., G. Wei, H. Fang, J. Guo, M. Weinstein, C. B. Marsh, M. C. Ostrowski, and S. Tridandapani. 2004. The inositol 3-phosphatase PTEN negatively regulates Fc gamma receptor signaling, but supports Toll-like receptor 4 signaling in murine peritoneal macrophages. *J. Immunol.* 172: 4851–4857.
27. Schabbauer, G., U. Matt, P. Günzl, J. Warszawska, T. Furtner, E. Hainzl, I. Elbau, I. Mesteri, B. Doninger, B. R. Binder, and S. Knapp. 2010. Myeloid PTEN promotes inflammation but impairs bactericidal activities during murine pneumococcal pneumonia. *J. Immunol.* 185: 468–476.
28. Sarraj, B., S. Massberg, Y. Li, A. Kasorn, K. Subramanian, F. Loison, L. E. Silberstein, U. von Andrian, and H. R. Luo. 2009. Myeloid-specific deletion of tumor suppressor PTEN augments neutrophil transendothelial migration during inflammation. *J. Immunol.* 182: 7190–7200.
29. Li, Y., Y. Jia, M. Pichavant, F. Loison, B. Sarraj, A. Kasorn, J. You, B. E. Robson, D. T. Umetsu, J. P. Mizgerd, et al. 2009. Targeted deletion of tumor suppressor PTEN augments neutrophil function and enhances host defense in neutropenia-associated pneumonia. *Blood* 113: 4930–4941.
30. Subramanian, K. K., Y. Jia, D. Zhu, B. T. Simms, H. Jo, H. Hattori, J. You, J. P. Mizgerd, and H. R. Luo. 2007. Tumor suppressor PTEN is a physiologic suppressor of chemoattractant-mediated neutrophil functions. *Blood* 109: 4028–4037.
31. Choi, J. S., H. J. Park, H. Y. Kim, S. Y. Kim, J. E. Lee, Y. S. Choi, M. H. Chun, J. W. Chung, and M. Y. Lee. 2005. Phosphorylation of PTEN and Akt in

astrocytes of the rat hippocampus following transient forebrain ischemia. *Cell Tissue Res.* 319: 359–366.

32. Howitt, J., J. Lackovic, L. H. Low, A. Naguib, A. Macintyre, C. P. Goh, J. K. Callaway, V. Hammond, T. Thomas, M. Dixon, et al. 2012. Ndfip1 regulates nuclear Pten import in vivo to promote neuronal survival following cerebral ischemia. *J. Cell Biol.* 196: 29–36.

33. Wu, J., J. Li, H. Hu, P. Liu, Y. Fang, and D. Wu. 2012. Rho-kinase inhibitor, fasudil, prevents neuronal apoptosis via the Akt activation and PTEN inactivation in the ischemic penumbra of rat brain. *Cell. Mol. Neurobiol.* 32: 1187–1197.

34. Guo, J. Y., J. Ding, F. Yuan, H. Chen, S. W. Chen, and H. L. Tian. 2013. Dose-Dependent Protective Effect of Bisperoxovanadium against Acute Cerebral Ischemia in a Rat Model of Ischemia/Reperfusion Injury. *Int. J. Mol. Sci.* 14: 12013–12022.

35. Wu, D. N., D. S. Pei, Q. Wang, and G. Y. Zhang. 2006. Down-regulation of PTEN by sodium orthovanadate inhibits ASK1 activation via PI3-K/Akt during cerebral ischemia in rat hippocampus. *Neurosci. Lett.* 404: 98–102.

36. Shi, G. D., Y. P. OuYang, J. G. Shi, Y. Liu, W. Yuan, and L. S. Jia. 2011. PTEN deletion prevents ischemic brain injury by activating the mTOR signaling pathway. *Biochem. Biophys. Res. Commun.* 404: 941–945.

37. Carini, R., M. Grazia De Cesaris, R. Splendore, G. Baldanzi, M. P. Nitti, E. Alchera, N. Filigheddu, C. Domenicotti, M. A. Pronzato, A. Graziani, and E. Albano. 2004. Role of phosphatidylinositol 3-kinase in the development of hepatocyte preconditioning. *Gastroenterology* 127: 914–923.

38. Dal Ponte, C., E. Alchera, A. Follenzi, C. Imarisio, M. Prat, E. Albano, and R. Carini. 2011. Pharmacological postconditioning protects against hepatic ischemia/reperfusion injury. *Liver Transpl.* 17: 474–482.

39. Horie, Y., A. Suzuki, E. Kataoka, T. Sasaki, K. Hamada, J. Sasaki, K. Mizuno, G. Hasegawa, H. Kishimoto, M. Iizuka, et al. 2004. Hepatocyte-specific Pten deficiency results in steatohepatitis and hepatocellular carcinomas. *J. Clin. Invest.* 113: 1774–1783.

40. Stiles, B., Y. Wang, A. Stahl, S. Bassilian, W. P. Lee, Y. J. Kim, R. Sherwin, S. Devaskar, R. Lesche, M. A. Magnuson, and H. Wu. 2004. Liver-specific deletion of negative regulator Pten results in fatty liver and insulin hypersensitivity [corrected]. [Published erratum appears in 2004. *Proc. Natl. Acad. Sci. USA* 101: 5180.] *Proc. Natl. Acad. Sci. USA* 101: 2082–2087.

41. Zhang, M. Z., B. Yao, S. Yang, L. Jiang, S. Wang, X. Fan, H. Yin, K. Wong, T. Miyazawa, J. Chen, et al. 2012. CSF-1 signaling mediates recovery from acute kidney injury. *J. Clin. Invest.* 122: 4519–4532.

42. Takeda, Y., S. Costa, E. Delamarre, C. Roncal, R. Leite de Oliveira, M. L. Squadrito, V. Finisguerra, S. Deschoemaeker, F. Bruyère, M. Wenes, et al. 2011. Macrophage skewing by Phd2 haplodeficiency prevents ischaemia by inducing arteriogenesis. *Nature* 479: 122–126.

43. Lee, S., S. Huen, H. Nishio, S. Nishio, H. K. Lee, B. S. Choi, C. Ruhrberg, and L. G. Cantley. 2011. Distinct macrophage phenotypes contribute to kidney injury and repair. *J. Am. Soc. Nephrol.* 22: 317–326.

44. Byles, V., A. J. Covarrubias, I. Ben-Sahra, D. W. Lamming, D. M. Sabatini, B. D. Manning, and T. Horng. 2013. The TSC-mTOR pathway regulates macrophage polarization. *Nat. Commun.* 4: 2834.

45. Arranz, A., C. Doxaki, E. Vergadi, Y. Martinez de la Torre, K. Vaporidi, E. D. Lagoudaki, E. Ieronymaki, A. Androulidaki, M. Venihaki, A. N. Margioris, et al. 2012. Akt1 and Akt2 protein kinases differentially contribute to macrophage polarization. *Proc. Natl. Acad. Sci. USA* 109: 9517–9522.